

1 **Landscape transformation processes in two large and two small cities in Egypt and**
2 **Jordan over the last five decades using remote sensing data**

3

4 **Abstract**

5 Much research has tackled the physical expansion of urban growth and concomitant rural-
6 urban transformation of land use in many parts of the world, but this phenomenon remained
7 largely overlooked in the Middle East and North Africa (MENA) region. To fill this
8 knowledge gap, this study investigated land use changes from the 1970s to 2018 in the cities
9 of Luxor and Cairo in Egypt and of Aqaba and Amman in Jordan using different Landsat
10 datasets. Land cover classifications were performed with Maximum Likelihood Algorithm
11 and Spectral Angle Mapper. In all four cities peri-urban green areas shrunk or shifted due to
12 increased expansion of built-up areas. The largest reduction of peri-urban green areas were
13 observed for Amman and Luxor, which decreased by 122.4 km² and 17.2 km², respectively,
14 over the study period. For Cairo, an increase of peri-urban green area by 29 km² was
15 detected, but its location shifted over the last five decades due to urban expansion. Green
16 areas (urban and peri-urban) on a per-capita basis were 4.6, 12, 91, and 142 m²/capita for
17 Aqaba, Cairo, Amman, and Luxor, respectively, in 2018. Land cover changes reflected
18 critical political events like the so-called “Arab Spring”, international treaties, recent
19 migration waves and population growth. Rapid increases in urban built-up area put pressure
20 on scarce land and water resources in the peri-urban fringes, thereby potentially leading to
21 environmental stress. Effective city planning is needed to address the multiple challenges and
22 competing interests of urban and peri-urban environments.

23

24 **Keywords:** Landsat images; Land use and land cover; MENA; Peri-urban green areas; Rural-
25 urban transition; Water and food shortage.

26 **1. Introduction**

27 Urban growth leads to land use and land cover changes in and around agglomerations. These
28 changes are particularly large in many poor countries characterized by rapid population
29 growth (UN-Habitat, 2014). Urban expansion is not limited to large metropolitan areas, but it
30 equally occurs in mid-sized and small cities (Gouda et al., 2016). The expansion of urban
31 areas challenges the continued existence of cropland, and specifically the growth of small and
32 medium sized settlements on the periphery of metropolitan areas may jeopardize local food
33 security (Robson et al., 2012; Seto & Ramankutty, 2016). Since urban water demands rise,
34 also competition for water is increasing between urban and agricultural sectors (Flörke et al.,
35 2018).

36 On a local scale, urban and peri-urban agriculture (UPA) plays an important role for
37 food security, income generation and recycling of waste, which has been well documented
38 (Levasseur et al., 2007; Prain and Lee-Smith, 2010). Whereas UPA was widely studied in
39 regions such as sub-Saharan Africa, information on the extent of UPA in Middle East and
40 North Africa (MENA) cities remains scarce (Graefe et al., 2019). As this region is
41 characterized by low annual rainfall, it has a high fraction of irrigated cropland (peri-) urban
42 areas (Thebo et al., 2014).

43 In Egypt agricultural production entirely depends on the availability of irrigation
44 water but increasingly also on the encroachment of urban settlements into arable land
45 (UNDP, 2009; Lenney et al., 1996). In the Greater Cairo Metropolitan Region most open
46 areas are now engulfed by highways and peripheral areas of surrounding villages, which led
47 to an increase of the city's urban area by 135 % between 1984 and 2013 (Osman et al.,
48 2016a,b). Similar changes were noted in Luxor, where agricultural land increased by about
49 1,940 ha from 1987 to 2011 (Ahmed et al., 2013).

50 In their analysis of spatial and temporal urban expansion on agricultural land for the
51 Greater Amman Municipality (Jordan) Al-Kofahi et al. (2018) found that it had declined by
52 50 % from 2003 to 2015. However, 14 % of Greater Amman still classifies as agricultural
53 land where strong municipal support has encouraged the development of UPA (Tawk et al.,
54 2011; Al-Kofahi et al., 2018). Al Farajat (2001) stated that Aqaba has become important for
55 heavy industry, as a free trade zone and for tourism, resulting in rapid urbanization. This
56 change in land use has led to major groundwater pollution from human and industrial
57 sources.

58 Urban growth using Landsat data has been widely studied in India (Wakode et al.,
59 2013; Bhatta, 2009; Jat et al., 2008), the US (Masek et al., 2000; Sexton et al., 2013), as well

60 as other regions (Bagan and Yagamata, 2012; Kaya and Curran, 2006). In the Middle East
61 research focused on the Gulf countries, such as Saudi Arabia (Rahman 2016; Alqurashi et al,
62 2016), the UAE (Yagoub, 2004), and Kuwait (Kwarteng and Chavez, 1998). However,
63 comparative studies on urban growth dynamics within one region are scarce, and particularly
64 the eastern MENA region has been rarely studied. To interpret rural-urban transformation
65 there, it is important to consider the broader political context shaping dynamics in urban
66 growth and cultivated areas. The so-called “Arab Spring” for instance affected enforcement
67 of land use and building regulations in Egypt. Due to conflicts and geopolitical instability, the
68 MENA region received several waves of refugees as a consequence of wars in neighbouring
69 countries. This needs particular attention when studying landscape transformation processes.
70 Sudden increase in population due to forced migration often results in increased water
71 demand, thus diverting water from the agricultural sector towards municipal and drinking
72 purposes. Given the low precipitation rates in the region, a sudden increase in population,
73 accompanied by increased food demand, does not directly lead to increased agricultural
74 production, as food policies need to match water policies. Therefore it is necessary to situate
75 the analysis of land transformation in the biophysical context of water resources scarcity.

76 In view of the rapid rural-urban transformation in MENA cities, the main objective of
77 this study was to quantify patterns of urban expansion and its effects on agricultural land
78 from the 1970s to 2018 for four MENA cities differing in size and growth dynamics. For this
79 purpose GIS-based remote sensing analysis was employed using different tools in ERDAS
80 IMAGINE 2014 and open source approaches implemented in QGIS and R.

81

82

83 **2. Methods**

84 **2.1. Study areas**

85 For the present study, we selected a major and a minor city each in two MENA countries,
86 Cairo and Luxor in Egypt, and Amman and Aqaba in Jordan (Fig. 1+2). Cairo, Luxor, and
87 Aqaba share the common characteristics of a hot desert climate with low annual rainfall,
88 mean temperatures $> 20^{\circ}\text{C}$, and location at altitudes < 100 m asl. Amman is characterized by
89 a slightly cooler and more humid climate due to its location at an altitude of 860 m asl (Table
90 1).

91 Cairo is the capital of Egypt and with 9,570,400 inhabitants in 2017 the country’s
92 largest city. Its metropolitan area is with 3,085 km² one of the biggest in Africa and the
93 largest in the MENA region and the Arab world. Luxor, in contrast, is located on the Eastern

94 bank of the Nile River in southern Egypt at a distance of 670 km from Cairo. In 2012, the
95 population of Luxor was 506,588, but increased to 1,300,000 in 2018, whereas the urban area
96 remained equal with approximately 714 km². Luxor's main activities are tourism and
97 agriculture, whereby 95 % of Luxor's water is consumed by the agricultural sector (Ahmed et
98 al., 2013).

99 Amman is the capital and most populous city of Jordan. In 2017, it had 4,007,500
100 inhabitants on a land area of 1,680 km², while the governorate of Amman comprises an area
101 of 7,579 km². Aqaba is the only coastal city in Jordan and the administrative centre of the
102 Aqaba Governorate. In 2017, the city had a population of 198,500 and a land area of 375 km²
103 (<http://dosweb.dos.gov.jo/>), which is partly occupied by an industrial free trade zone, but also
104 for tourism.

105 [Table 1, Fig. 1+2 near here]

106

107 **2.2. Data acquisition and pre-processing**

108 The official administrative boundaries of the study areas were imported as shapefiles
109 from the spatial database provided by DIVA-GIS (<http://www.diva-gis.org/gdata>) into QGIS
110 2.18.18. Some enhancements and corrections were required on the city boundaries based on
111 recent google maps, which were used as a background in the QGIS working space. Google
112 maps were generated after installing OpenLayers plugin to QGIS. Initial image inspection
113 revealed that the obvious areas of rural-urban transformation were much smaller than the
114 cities' total areas, given that the remaining area consists of desert, barren land or mountains.
115 Hence, the area analysed from each city was visually selected to be within the cities'
116 administrative boundaries and to cover at least twice the area where the rural urban
117 transformation happened until 2018. These study boundaries were kept constant for image
118 processing, classifications and analysis across years.

119 The USGS Global Visualization Viewer (GloVis; <https://glovis.usgs.gov/>) server was
120 used to download Landsat 4-5 Thematic Mappers (TM) for images of the 1980s, 1990s and
121 early 2000s, and Landsat 8 Operational Land Imager (OLI) and Thermal Infrared Sensor
122 (TIRS) database for the most recent images of 2018 (Table 2). All images used in this study
123 are from the agricultural summer period (March - August) during which zero cloud cover
124 allowed for high image quality. During this period, all green areas were clearly visible in both
125 countries. In Egypt, agricultural activities are continuing throughout the entire year, due to
126 the well-established irrigation infrastructure following the High Aswan Dam construction in
127 1970 (Abu-Zeid, 1997). In Amman green areas increase after the rainy season (from

128 November to May) and in Aqaba green areas are irrigated year round by municipal treated
129 wastewater and groundwater (Al Farajat, 2001).

130 [Table 2 near here]

131

132 **2.3 Image classification and accuracy assessment**

133 *2.3.1 Supervised classification using Maximum Likelihood Algorithm*

134 All image bands (except thermal bands) were stacked and subsets manually clipped according
135 to the study areas' predefined boundaries. Subsequently, a Supervised Maximum Likelihood
136 classification (MLC) was applied by using Earth Resource Data Analysis System (ERDAS)
137 IMAGINE 2014 for all study areas. The maximum likelihood algorithm is based on the
138 likelihood that each pixel belongs to a particular class. It assumes that (i) likelihoods are
139 equal for all classes, (ii) input bands are uniformly distributed, and (iii) data is normally
140 distributed in each band of the classification (Vorovencii & Muntean, 2013). To double check
141 classification results a code was created in RStudio, which is exemplarily shown for Luxor
142 2000 (Appendix A).

143 A total of 24 signature files were created for the classification training of all study areas
144 across all years of analysis. The general land cover classes were "Urban", "Urban+Green"
145 (buildings with gardens and dense shrubs), "Peri-Urban Green" (agricultural lands, shrubs
146 and forests that are outside the urban region), "Barren lands", and "Deserts" and "Mountains"
147 (Table 3). We thereby defined „Peri-Urban Green“ as areas covered by vegetation
148 (agricultural lands, shrubs and forests) that are outside of but directly adjacent to built-up
149 areas. We deliberately omitted a "rural" land cover class from our analysis, since due to the
150 arid climate prevailing throughout the year no transition from peri-urban to rural areas is
151 visible, but instead we observe an abrupt (almost digital) change from built-up areas and/or
152 peri-urban green to land cover classes "Desert/barren" and "Mountain/barren". In addition,
153 historical demographic data of the four cities was collected to relate the share of the land
154 cover classes to a per capita basis (dosweb.dos.gov.jo; <http://egypt.opendataforafrica.org/>).

155 [Table 3 near here]

156

157 *2.3.2. Supervised classification using Semi-Automatic Classification Plugin (SCP) on QGIS*

158 The Semi-Automatic Classification Plugin (SCP) is a free open source plugin for
159 QGIS that allows to carry out supervised and unsupervised classification of remote sensing
160 images (Congedo, 2016). The Spectral Angle Mapper (SAM) algorithm was used in the
161 Supervised classification by SCP to compare its classification results with the Maximum

162 Likelihood Classification (MLC) made by ERDAS IMAGINE and R. The Spectral Angle
163 Mapper (SAM) is based on identifying pixel spectra through its angular information only.
164 The length of the vector increases or decreases according to the overall illumination
165 (increases or decreases due to the presence of sunlight or shadows), but its angular orientation
166 will remain constant. Two features match if the angle is smaller than a specified tolerance
167 value (Kruse et al., 1993).

168

169 2.3.3. Normalized difference vegetation index (NDVI)

170 The Normalized Difference Vegetation Index (NDVI) was applied as an additional
171 tool to detect green areas in Aqaba. This city has very limited green areas with weak
172 vegetation cover, which were hardly recognized by automatic classification and visual
173 inspection. The NDVI was calculated using Band 4 for NIR and Band 3 for Red from
174 Landsat 4-5. NDVI calculations were performed with R. For the code of Aqaba 2000 please
175 refer to Appendix B.

176 The NDVI quantifies vegetation by measuring the difference between near-infrared
177 (which vegetation strongly reflects) and red light (which vegetation absorbs). Healthy
178 vegetation (chlorophyll) reflects more near-infrared (NIR) and green light than other
179 wavelengths, but it absorbs more red and blue light. The NDVI is calculated from these
180 individual measurements as follows:

$$181 \quad \text{NDVI} = \frac{\text{NIR} - \text{Red}}{\text{NIR} + \text{Red}} \quad \text{Equation 1}$$

182 where NIR and red stand for the spectral reflectance measurements acquired in the near-
183 infrared and the red (visible) regions, respectively (GISGeography, 2018). Negative values of
184 NDVI correspond to water. NDVI values close to zero (-0.1 to 0.1) generally correspond to
185 barren areas of rock, sand, or snow. Lastly, low, positive values represent shrub and grassland
186 (approximately 0.2 to 0.4), while high values indicate high dense vegetation like temperate
187 and tropical rainforests (values approaching 1; NASA, 2000).

188

189 2.3.4. Change detection and post-classification

190 For change detection, we applied the post-classification comparison as previously described
191 by Singh et al. (1989), Paolini et al. (2006) and Brinkmann et al. (2011). It is based on
192 overlaying two or more independently produced spectral classification results, whereby
193 change areas are identified from one image to another taken at a different time. An analysis
194 of cross-tabulation was performed to project the land transformation in each city. Accuracy of

195 the classified maps was only determined by Kappa coefficients and overall accuracy. To
196 avoid possible biases in post-classification comparison resulting from different spatial
197 resolutions, visual on-screen interpretation with reference maps along with the automatic
198 classification on all landsat images series were applied (Ruelland et al., 2010).

199

200 3. Results

201 3.1. Luxor

202 In the 1970s the urban area of Luxor had an extent of only 3.1 km² and was largely limited to
203 the Eastern bank of the Nile River, surrounded by large agricultural areas extending over 192
204 km². Urban areas gradually emerged on the Eastern and Western banks of the Nile River (Fig.
205 6a+b), and increased to 91 km² by 2018 (encompassing 0.5% of the total area of interest in
206 1975, but more than >15% in 2018). From 1975 to 2000 a decrease in agricultural areas was
207 observed and new cultivated areas in the deserts were developed. From 2011 to 2018,
208 apparent urbanization rates increased again, which was accompanied by a reduction of
209 agricultural areas of 2% (Fig. 8a+b). From 1975 to 2018, agricultural areas in the
210 surroundings of Luxor decreased by 793 ha. Most urban expansion occurred into desert areas.

211 While the city grew into the former peri-urban zone, new cultivated areas emerged in
212 the peri-urban fringes at the border with the desert, especially after 1994, the year of the New
213 Esna Barrage inauguration (Ahmed et al., 2013) which was constructed on the Nile River 90
214 km upstream of Luxor city, and replaced the old Esna Barrage to control and improve the
215 performance of water distribution and to cover increasing needs for water (El Gamal et al.,
216 2007). The total peri-urban green area is not representative for the overall land transformation
217 processes, as newly cultivated areas substituted part of the peri-urban areas lost by
218 urbanization. To better understand this replacement process, change detection was used to
219 quantify green area changes within the administrative city boundary (Fig. 1), comprising
220 urban and peri-urban areas (Fig. 3). From 1990 to 2011, around 94.5 km² were cultivated in
221 the peri-urban zone. In 1984 arable lands in Luxor had only very little vegetation, which
222 reflected the Nile River's low flow during this period, as a consequence of the severe drought
223 in the Nile Basin countries between 1978 to 1987. However, in our study these areas were
224 classified as agricultural, not barren lands.

225 To validate the accuracy of the analytical procedures, a Spectral Angle Mapper
226 (SAM) algorithm by QGIS-SCP and the Maximum Likelihood Classification (MLC)
227 implemented in R were used in the classification process for Luxor 2000 (Fig. 4). The
228 analysis showed a very good agreement between MLC and SAM algorithms, as the
229 accuracies were 98 % for the desert, 94 % for the green and 97 % for the urban landcover
230 class.

231 [Fig. 3 + 4 near here]

232

233

234 **3.2. Cairo**

235 The urban area of Cairo had an extent of only 47.5 km² in 1972, but increased by 887 km²
236 over the next 46 years, resulting in an urban area of 935 km² in 2018. This expansion took
237 mainly place on barren land, which decreased by 1,079 km² during the same period. Urban
238 green areas extended over 99 km² in 1972, which increased to 256 km² in 2018. This
239 corresponds to 2.6-fold increase of urban green areas, compared to a nearly 20-fold increase
240 of urban (built-up) area.

241 Agricultural areas (peri-urban green) increased by 29 km² during the study period,
242 which were in 1970s mainly concentrated in the north-western area of Cairo. This zone
243 became gradually urbanized, and peri-urban green areas completely disappeared at this site
244 until 2011. In the meantime, however, a new peri-urban green area in the north of Cairo
245 appeared, which is clearly visible in the satellite image of 2018 (Fig. 6c+d). In general, peri-
246 urban green areas of Cairo are very limited, and ranged from 3 % (84.4 km²) in 1972 to
247 around 4 % (113.3 km²) in 2018, in relation to the total area of interest (Fig. 8d). Urban areas
248 in contrast increased from 1.6 % in 1972 to more than 32 % in 2018, resulting in urbanization
249 rates of around 133% from 2000 to 2011, and 200% from 2011 to 2018 (Fig. 8e).

250 [Fig. 6 + 8 near here]

251

252 **3.3. Aqaba**

253 The area of interest for Aqaba amounts to 168.1 km². Urban areas increased from 1 km² in
254 1975 to 43.1 km² in 2018. This expansion took mainly place on barren land, but also peri-
255 urban green areas decreased by 325 ha during the same period. Peri-urban green areas in
256 Aqaba were very restricted during the entire study period (Fig. 7a+b). The highest extent of
257 peri-urban green areas was observed in 2000, with a share of 4% of the total area (634 ha),
258 which decreased to 0.5% (92 ha) in 2018 as a consequence of urbanization. Sudden increases
259 in urbanization rates accompanied by decreases in green areas were noticed after 2000 and
260 2011 (Fig. 9a+b).

261

262 **3.4. Amman**

263 The area of interest for Amman has a size of 1,760.1 km². Woodlands and shrubs in the north
264 and west, agricultural lands in the south, and barren lands and mountains in the east surround
265 the urban area of Amman (Fi. 7c+d). The urban area occupied 12.8 km² in 1984, and
266 increased by 281 km² until 2018. Urban green areas in contrast increased by only 125 ha

267 during the same period, whereas peri-urban agricultural areas were reduced by 122 km².
268 Urbanization rates in Amman were most pronounced in the late 1990s (Fig. 9d+e).

269 The growth patterns of the city of Amman are similar to Luxor, as in both cities peri-
270 urban green areas were replaced by urban areas, while at the same time new cultivated lands
271 emerged at different locations. For this reason, an area change detection was applied for the
272 peri-urban green zone of Amman. From 2000 to 2011 a vast expansion in urban and
273 cultivated lands occurred (Fig. 5).

274 [Fig. 5; 7; 9 near here]

275

276 **3.5. Comparing urbanization dynamics of the four cities**

277 Our study showed that the larger the city the larger the absolute increase of the urban area
278 over the last decades. The land cover class “urban green” was only detected in the two larger
279 cities, Cairo and Amman, whereas it does not seem to play a major role in Luxor and Aqaba.
280 Before the 21st century urban green areas dominated over urban built-up areas in Cairo and
281 Amman, whereas from 2000 onwards a transition towards a reduction in urban green space
282 took place, which decreased to 30% and below until 2018.

283 Peri-urban green (which is partly composed of peri-urban gardens and agriculture, but
284 may also comprise shrubs and forests) has the largest areal extent in Amman (382 km² in
285 2018) and Luxor (183.9 km² in 2018). In Luxor, peri-urban green occupies as twice as much
286 space as the urban built-up area, and in Amman, it occupies 90% of the urban built-up area.
287 In Cairo and Aqaba in contrast, peri-urban green occupies only a size of 10% and 2%,
288 respectively, of the total urban area. The strongest decrease (in absolute values) of the
289 agricultural area was observed for Amman, which decreased by 122.4 km² from 1984 to
290 2018. For Luxor a reduction of 17.2 km² and for Aqaba of 3.3 km² was estimated for the
291 same time period, whereas it increased in Cairo.

292 Historical demographic data of the four cities was collected to relate the share of the
293 land cover classes “peri-urban green” and “urban green” to a per capita basis (Fig. 8 c+f, Fig.
294 9 c+f). The analysis showed that green areas per capita declined dramatically over the study
295 period. For 2018 values were lowest for Aqaba with 4.6 m²/capita and Cairo with 12
296 m²/capita. In Amman it dropped from 500 m²/capita in 1975 to < 91 m²/capita in 2018 and in
297 Luxor from 2,070 m²/capita to < 142 m²/capita during the same period.

298

299

300

301 **4. Discussion**

302 **4.1 Methods and tools used for satellite image classification**

303 The two approaches, Maximum likelihood classification (MLC) applied in ERDAS
304 IMAGINE 2014 and R coding and Spectral Angling Mapping (SAM) algorithm implemented
305 in QGIS-SCP yielded similar classification results. This may be expected when pixel spectra
306 from different classes are well distributed in feature space with uniform illumination, which
307 was the case in the images with zero clouds. It also leads to a high likelihood that angular
308 information alone provides good separation (Richards, 1999). All of our images could be
309 accurately classified. Some error confusion only occurred in the images of the 1970s
310 (especially for Aqaba 1975), which was most likely due to a poor resolution and hardly
311 distinguishable colours of mountains, barren lands, and roads. For most of the images the
312 overall classification accuracy was higher than 95 % and Kappa coefficients were higher than
313 0.91.

314

315 **4.2. Land cover changes over the last five decades and their drivers**

316 Growth of built-up areas occurs mostly along major transportation systems, and
317 cropland is one of the most affected land uses through urban growth (Bagan & Yamagata,
318 2012; Wakode et al., 2014). Dynamics of urbanization and urban growth in developing
319 countries are usually linked to demographic factors (Jedwab et al., 2017). Many driving
320 forces of land use changes are well documented (Lambin et al., 2001), but interpretation
321 remains difficult, since it is the result of many often interacting factors including population
322 growth and climate variability (Leblanc et al., 2007). Political, social and economic reasons
323 are playing important roles in land use changes (Hersperger et al., 2018).

324 Urbanization rates were highest for Cairo and Aqaba, the largest and smallest cities in
325 this study. In both cities, urban expansion mostly occurred on desert areas, which was the
326 dominating land cover class outside the cities. However, in the Nile delta urban expansion
327 also occurred on highly fertile soils (Shalaby & Moghanm, 2015). Spatial patterns of urban
328 growth in Cairo mainly followed transportation corridors (Hou et al., 2016). Luxor and
329 Amman share similar land transformation processes. Urban encroachment mainly occurred
330 into the peri-urban green areas, whereas cultivation and/or degradation of agricultural/green
331 areas could be observed in the transition zone from the peri-urban space to the desert.
332 Between 1990 and 2011, and especially after the construction of New Esna Barrage in 1994,
333 Luxor gained around 94.5 km² of cultivated lands at the peri-urban fringe, but at the same
334 time lost around 37 km² (Fig. 9 a+b). Amman had around 120 km² of cultivated land at the

335 peri-urban fringe between 2000 and 2011, but in the meantime lost almost the same area (Fig.
336 9d+e). Encompassing a larger time span than our study, Al Rawashdeh & Saleh (2006)
337 estimated that Amman lost 23% of its fertile land between 1918 and 2002.

338 New water projects can help to compensate urbanization-related losses of agricultural
339 areas, as it became evident for Luxor through the construction of the New Esna Barrage in
340 1994. This led to the cultivation of new land outside the city. It is well known that the
341 extension of roads and infrastructure plays a considerable role for urban agglomerations
342 (Fang & Yub, 2017). Another main driver for the Egyptian case study cities was the so called
343 “Arab Spring”, which started in 2011, and is considered one of the main political and social
344 reasons for the sudden increase in the urbanization rates and the concomitant decline of the
345 peri-urban agricultural/green areas in Cairo and Luxor after 2011 (Khamis et al., 2015).
346 During this period governmental authorities lost control, hence many people grabbed the
347 chance and converted irrigated agricultural land into housing areas.

348 In Amman and Aqaba urbanization rates increased rapidly after 2000. Especially in
349 Amman, this sudden increase can be related to the migration of refugees from areas of
350 conflict such as Palestine (UNRWA, 2019), while refugees from Iraq came to Jordan after the
351 2003 Iraq war, and from Syria after 2011.

352 Between 2011 and 2018 agricultural and green areas in Amman and Aqaba declined
353 rapidly. Drivers for Amman may be rapid urbanization and climate change, for Aqaba’s
354 development political decisions such as the 2015 agreement on management and utilization
355 of the ground water in the Disi-Saq Aquifer between Jordan and Saudi Arabia were certainly
356 important (Eckstein, 2015). Jordan seems to have sufficient productive areas available to
357 buffer the effects of urban expansion on food production for the next decades, but effects of
358 climate change may still result in an increase in irrigation requirements and cropland area
359 (Koch et al., 2018).

360

361 **4.3. Implications of urbanization for food security, urban agriculture and waste** 362 **management**

363 Several authors provide evidence that urban agglomerations largely depend on food
364 produced outside urban and peri-urban areas (Drechsel et al., 2007; Porter et al., 2014; Zhou
365 et al., 2012). Studies on geographical sources supplying food to urban centers, however, are
366 scarce, which particularly refers to the MENA region. Both Egypt and Jordan highly depend
367 on food imports, and are thus vulnerable to increasing food prices (Veninga & Ihle, 2018). In
368 2016, per capita imports of wheat, the most important staple crop in the region, were around

369 90 and 200 kg year⁻¹ for Egypt and Jordan, respectively (Fig. 10). Per-capita wheat imports
370 strongly increased in both countries in the late 70s, which can be mainly attributed to changes
371 in the diet and population increase.

372 Urbanization creates new markets, and growing urban areas are important sales
373 market for intensive peri-urban vegetable production (FAO, 2011). The importance of UPA
374 to provide cities with fresh produce is very context-specific. For Egypt, a rather low success
375 of urban agriculture and lacking institutional frameworks has been documented (Tawk et al.,
376 2011). In Cairo crop production is rather confined to peri-urban areas, but can be also found
377 in informal settlements. A contrasting picture was reported from Amman, where a high share
378 of the land remains uncovered by buildings and is thus still available for agriculture (Tawk et
379 al., 2011). Due to its market proximity the main target of UPA, however, is to supply cities
380 with high value perishable fruits and vegetables, rather than staple crops.

381 Urban centers are strong nutrient sinks through the obviously high amount of food
382 inflows, whereas rural areas export nutrients (Drechsel et al., 2007; Karg et al., 2016). The
383 same applies for virtual water flows from production to consumption regions, which refers to
384 the amount of water needed for the production of food commodities (Hoff et al., 2014;
385 Akoto-Danso et al., 2019). To minimize environmental pollution and reduce waste loads an
386 efficient municipal waste management is required. In this context, UPA has a well-known
387 potential to absorb part of the solid and liquid waste accumulating in urban centers (Faruqui
388 et al., 2008; Grard et al., 2015; Al-Ismaili et al., 2017). In many cases, however, areas
389 designated for UPA heavily compete with other claims, such as for construction and housing.
390 Competition does not only exist for space, but also for water, especially in water scarce
391 regions such as MENA, since urban water demands are increasing (Flörke et al., 2018).
392 Particularly in dry areas, growing cities will have priority for water supply, thereby reducing
393 available water for agriculture, which leads to further losses of agricultural land (FAO, 2011).
394 This pressure on resources became also evident in the present study, which highlighted
395 decreasing green space in the cities of Cairo and Amman, and a partial displacement or shift
396 of peri-urban green areas.

397 [Fig. 10 near here]

398

399 **4.4. Existing initiatives to overcome land and water scarcity**

400 In view of the rapid transformation processes in urban and peri-urban areas of the
401 study region, new options for non-traditional sources of water and land are needed. UN-
402 Habitat proposes to minimize urban expansion by encouraging densification and development

403 of more compact cities (Seto & Ramankutty, 2016). Egypt and Jordan already started
404 constructing new plants for seawater desalination and reclaiming new areas to cover the
405 growing future needs. In 2015, Egypt launched a national project for constructing new
406 communities and reclaiming 6,070 km² in the western desert and Sinai. Groundwater from
407 The Nubian Sandstone Aquifer will be the main source for irrigation and domestic purposes.
408 In March 2017, a new seawater desalination plant was inaugurated in Aqaba to produce
409 around 5 million m³ clean water annually for drinking, agricultural, and industrial purposes.
410 This in turn will reduce the high rates of groundwater consumption in the Disi aquifer (The
411 Jordan Times, 2017). Jordan also signed a plan with Israel and Palestine for constructing the
412 Red-Dead Sea Pipeline Project, which envisions producing fresh water through desalination
413 (Josephs, 2013).

414

415 **5. Conclusions**

416 The current study shows that over the study period urbanization strongly affected land
417 cover changes in and around the four case study cities. In all cases it became evident that
418 peri-urban green areas had shrunk or shifted due to increased expansion of built-up areas.
419 Only in Cairo a slight increase of peri-urban green area was observed. Whereas the land
420 cover class “urban green” was non-existent in Luxor and Aqaba, it significantly decreased in
421 Cairo and Amman. It has to be noted that changes in sensor quality and image resolution
422 make time series analysis difficult when using landsat data for the detection of rural-urban
423 transformation processes. This is particularly true for peri-urban areas which are often
424 undergoing particularly dynamic transitions in space and structure. We have omitted this
425 problem by summarizing this space as “peri-urban green” comprising peri-urban gardens and
426 agricultural land. This may be justified for our study sites are they are surrounded by barren
427 desserts, but typically warrants more detailed attention elsewhere. In the future approaches
428 combining big data capabilities will allow likely to allow to fuse multi- and hyper-spectral
429 reflectance data with 3-D models of plant and built-up structures offering more dynamic
430 insights into the ecological consequences of land use and land cover changes.

431 Like elsewhere also in the four MENA cities of our study land use and land cover
432 changes are a result of the combination of different drivers, which include population growth
433 as well as political and economic reasons. Future research also comprising field surveys and
434 land reconnaissance studies may allow a better understanding of the underlying
435 environmental and socio-economic forces, which interact and lead to different effects on the
436 dynamics and patterns of urban, peri-urban and rural areas across the MENA countries. As

437 elsewhere effective city planning needs to address competing claims for housing and green
438 space and to recognize the role that UPA can play for food production, income provision,
439 waste recycling, and creation of green space.

References

- Abu-Zeid, M. (1997, September). Egypt's water policy for the 21st century. A special session on water management under scarcity conditions: the Egyptian experience. IXth World Water Congress of IWRA, Montreal, Canada.
- Ahmed, A., Fogg, G., & Gameh, M. (2013). Water use at Luxor, Egypt: Consumption analysis and future demand forecasting. *Environmental Earth Sciences*, 72(4), 1-14. <https://doi.org/10.1007/s12665-013-3021-8>
- Akoto-Danso, E., Karg, H., Drechsel, P., Nyarko, G. & Buerkert, A. (2019). Virtual water flow in food trade systems of two West African cities. *Agricultural Water Management*, 213, 760-772. <https://doi.org/10.1016/j.agwat.2018.11.012>
- Al Farajat M. (2001). Hydrogeo-Eco-Systems in Aqaba/Jordan – Coasts and region; Natural settings, impacts of land use, spatial vulnerability to pollution and sustainable management. PhD thesis, Julius-Maximilians-University of Würzburg, Germany.
- Al-Ismaïli, A.M., Ahmed, M., Al-Busaidi, A., Al-Adawi, S., Tandlich, R., & Al-Amri, M. (2017). Extended use of grey water for irrigating home gardens in an arid environment. *Environmental Science and Pollution Research*, 24, 13650-13658. <https://doi.org/10.1007/s11356-017-8963-z>
- Al-Kofahi, S. D., Hammouri, N., Sawalhah, M. N., Al-Hammouri, A. A., & Aukour, F. J. (2018). Assessment of the urban sprawl on agricultural lands of two major municipalities in Jordan using supervised classification techniques. *Arabian Journal of Geosciences*, 11, 45. <https://doi.org/10.1007/s12517-018-3398-5>
- Al Rawashdeh, S., & Saleh, B. (2006). Satellite monitoring of urban spatial growth in the Amman area, Jordan. *Journal of Urban Planning and Development*, 132(4), 211-216. [https://doi.org/10.1061/\(ASCE\)0733-9488\(2006\)132:4\(211\)](https://doi.org/10.1061/(ASCE)0733-9488(2006)132:4(211))
- Alqurashi, A., Kumar, L., & Sinha, P. (2016). Urban land cover change modelling using time-series satellite images: A case study of urban growth in five cities of Saudi Arabia. *Remote Sensing*, 8(10), 838.
- Bagan, H., & Yamagata, Y. (2012). Landsat analysis of urban growth: How Tokyo became the world's largest megacity during the last 40 years. *Remote Sensing of Environment*, 127, 210-222.
- Bhatta, B. (2009). Analysis of urban growth pattern using remote sensing and GIS: a case study of Kolkata, India. *International Journal of Remote Sensing*, 30(18), 4733-4746.
- Brinkmann, K., Schumacher, J., Dittrich A., Kadaore I., & Buerkert, A. (2011). Analysis of landscape transformation processes in and around four West African cities over the last 50 years. *Landscape and Urban Planning*, 105(1-2), 94-105. <https://doi.org/10.1016/j.landurbplan.2011.12.003>
- Congedo, L. (2016). *Semi-automatic classification plugin documentation*. Release 6.0.1.1. <http://dx.doi.org/10.13140/RG.2.2.29474.02242/1>
- Drechsel, P., Graefe, S., & Fink, M. (2007). Rural-urban food, nutrient and virtual water flows in selected West African cities. *IWMI Research Report 115*. Colombo: International Water Management Institute.
- Eckstein, G. (2015). The newest transboundary aquifer agreement: Jordan and Saudi Arabia cooperate over Al-Sag/Al-Disi Aquifer. International Water Law Project Blog. <https://www.internationalwaterlaw.org/blog/2015/08/31/the-newest-transboundary-aquifer-agreement-jordan-and-saudi-arabia-cooperate-over-the-al-sag-al-disi-aquifer/> Accessed 09 April 2019.
- El Gamal, F., Hesham, M., & Shalaby, A. R. (2007). Country paper on harmonization and integration of water saving options in Egypt. In F. Karam, K. Karaa, N. Lamaddalena, & C. Bogliotti (Eds.), *Harmonization and integration of water saving options*. Convention

- and promotion of water saving policies and guidelines (pp. 81-90). Bari: CIHEAM/EU DG Research.
- Fang, C., & Yub, D. (2017). Urban agglomeration: An evolving concept of an emerging phenomenon. *Landscape and Urban Planning*, 162, 126-136. <https://doi.org/10.1016/j.landurbplan.2017.02.014>
- FAO (2011). The state of the world's land and water resources for food and agriculture (SOLAW) – Managing systems at risk. Food and Agriculture Organization of the United Nations, Rome and Earthscan, London.
- Faruqui, N., Al-Jayyousi, O. (2009). Greywater reuse in urban agriculture for poverty alleviation. A case study in Jordan. *Water International*, 27, 387-394. <https://doi.org/10.1080/02508060208687018>
- Flörke, M., Schneider, C., McDonald, R.I. (2018). Water competition between cities and agriculture driven by climate change and urban growth. *Nature Sustainability*, 1(1), 51–58. <https://doi.org/10.1038/s41893-017-0006-8>
- GISGeography (2018). What is NDVI (Normalized Difference Vegetation Index)? <https://gisgeography.com/ndvi-normalized-difference-vegetation-index/> Accessed 11 April 2019.
- Gouda, A. A., Hosseini, M., & Masoumi, H. E. (2016). The status of urban and suburban sprawl in Egypt and Iran. *GeoScape*, 10(1), 1-15. <https://doi.org/10.1515/geosc-2016-0001>
- Graefe, S., Buerkert, A., & Schlecht, E. (2019). Trends and gaps in scholarly literature on urban and peri-urban agriculture. *Nutrient Cycling in Agroecosystems*, 115(2), 143-158. <https://doi.org/10.1007/s10705-019-10018-z>
- Grard, B.J. - P., Bel, N., Marchal, N., Madre, F., Castell, J. - F., Cambier, P., Houot, S., Manouchehri, N., Besancon, S., Michel, J. - C., Chenu, C., Frascaria-Lacoste, N., & Aubry, C. (2015). Recycling urban waste as possible use for rooftop vegetable garden. *Future for Food: Journal on Food, Agriculture and Society*, 3, 21-34.
- Hersperger, A., Oliveira E., Pagliarin S., Palka G., Verburg P., Bolliger J., & Grădinarua S. (2018). Urban land-use change: The role of strategic spatial planning. *Global Environmental Change*, 51(7), 32-42. <https://doi.org/10.1016/j.gloenvcha.2018.05.001>
- Hoff, H., Döll, P., Fader, M., Gerten, D., Hauser, S. & Siebert, S. (2014). Water footprints of cities – indicators for sustainable consumption and production. *Hydrology and Earth System Sciences*, 18, 213-226. <https://doi.org/10.5194/hess-18-213-2014>
- Hou, H., Estoque R.C., & Murayama, Y. (2016). Spatiotemporal analysis of urban growth in three African capital cities: A grid-cell-based analysis using remote sensing data. *Journal of African Earth Science*, 123, 381-391. <https://doi.org/10.1016/j.jafrearsci.2016.08.014>
- Jat, M. K., Garg, P. K., & Khare, D. (2008). Modelling of urban growth using spatial analysis techniques: a case study of Ajmer city (India). *International Journal of Remote Sensing*, 29(2), 543-567
- Jedwab, R., Christiaensen, L., & Gindelsky M. (2017). Demography, urbanization and development: Rural push, urban pull and ... urban push. *Journal of Urban Economics*, 98, 6-16. <https://doi.org/10.1016/j.jue.2015.09.002>
- The Jordan Times (2017) Jordan's first water desalination plant opens in Aqaba. <http://www.jordantimes.com/news/local/jordan%E2%80%99s-first-water-desalination-plant-opens-aqaba> Accessed 09 April 2019.
- Josephs, J. (2013). Green light for Red-Dead Sea pipeline project. *Water & Wastewater International (WWi) Magazine*, 28(6). <https://www.waterworld.com/articles/wwi/print/volume-28/issue-6/technology-case-studies/water-provision/green-light-for-red-dead-sea-pipeline-project.html> Accessed 09 April 2019.

- Kaya, S., & Curran, P. J. (2006). Monitoring urban growth on the European side of the Istanbul metropolitan area: A case study. *International Journal of Applied Earth Observation and Geoinformation*, 8(1), 18-25.
- Karg, H., Drechsel, P., Akoto-Danso, E.K., Glaser, R., Nyarko, G., & Buerkert, A. (2016). Foodsheds and city region food systems in two West-African cities. *Sustainability*, 8(12), 1175. <https://doi.org/10.3390/su8121175>
- Khamis, R., Ali, A., & Hahn, M. (2015). Assessing the urban encroachment phenomenon in Egypt using satellite imagery. *International Journal of Scientific & Engineering Research*, 6(11), 1148-1159. ISSN 2229-5518
- Koch, J., Wimmer, F., & Schaldach, R. (2018). Analyzing the relationship between urbanization, food supply and demand, and irrigation requirements in Jordan. *Science of the Total Environment*, 636, 1500-1509. <https://doi.org/10.1016/j.scitotenv.2018.04.058>
- Kruse, F. A., Lefkoff, A. B., Boardman, J.W., Heidebrecht, K.B., Shapiro, A. T., Barloon, P.J., & Goetz, A. F. H. (1993). The spectral image processing systems (SIMS) – Interactive visualization and analysis of imaging spectrometer data. *Remote Sensing of Environment*, 44, 145– 163.
- Kwarteng, A. Y., & Chavez Jr, P. S. (1998). Change detection study of Kuwait City and environs using multi-temporal Landsat Thematic Mapper data. *International Journal of Remote Sensing*, 19(9), 1651-1662
- Lambin, E. F., Turner, B. L., Geist, H. J., Agbola, S. B., Angelsen, A., Bruce, J. W., Coomes, O. T., Dirzo, R., Fischer, G., Folke, C., et al. (2001). The causes of land-use and land-cover change: Moving beyond the myths. *Global Environmental Change*, 11(4), 261–269. [https://doi.org/10.1016/S0959-3780\(01\)00007-3](https://doi.org/10.1016/S0959-3780(01)00007-3)
- Leblanc, M. J., Favreau, G., Massuel, S., Tweed, S. O., Loireau, M., & Cappelaere, B. (2007). Land clearance and hydrological change in the Sahel: SW Niger. *Global and Planetary Change*, 61(3–4), 135–150. <https://doi.org/10.1016/j.gloplacha.2007.08.011>
- Lenney, M. P., Woodcock, C. E., Collins, J. B., & Hamdi, H. (1996). The status of agricultural lands in Egypt: the use of multitemporal NDVI features derived from Landsat TM. *Remote Sensing of Environment*, 56, 8-20. [https://doi.org/10.1016/0034-4257\(95\)00152-2](https://doi.org/10.1016/0034-4257(95)00152-2)
- Levasseur, V., Pasquini, M. W., Kouamé, C., & Temple, L. A. (2007). Review of urban and peri-urban vegetable production in West Africa. *Acta Horticulturae*, 762, 245-252. <https://doi.org/10.17660/ActaHortic.2007.762.23>
- Masek, J. G., Lindsay, F. E., & Goward, S. N. (2000). Dynamics of urban growth in the Washington DC metropolitan area, 1973-1996, from Landsat observations. *International Journal of Remote Sensing*, 21(18), 3473-3486.
- NASA (2000). Measuring Vegetation (NDVI & EVI). <https://earthobservatory.nasa.gov/features/MeasuringVegetation> Accessed 11 April 2019.
- Osman, T., Arima, T., & Divigalpitiya, P. (2016a). Measuring urban sprawl patterns in Greater Cairo Metropolitan Region. *Journal of the Indian Society of Remote Sensing*, 44(2), 287–295. <https://doi.org/10.1007/s12524-015-0489-6>
- Osman, T., Divigalpitiya, P., & Arima, T. (2016b). Quantifying the driving forces of informal urbanization in the Western part of the Greater Cairo Metropolitan Region. *Environments*, 3, 13. <https://doi.org/10.3390/environments3020013>
- Paolini, L., Grings, F., Sobrino, J. A., Jiménez Muñoz, J. C., & Karszenbaum, H. (2006). Radiometric correction effects in Landsat multi-date/multi-sensor change detection studies. *International Journal of Remote Sensing*, 27(4), 685-704. <https://doi.org/10.1080/01431160500183057>

- Porter, J. R., Dyball, R., Dumaresq, D., Deutsch, L., & Matsuda, H. (2014). Feeding capitals: Urban food security and self-provisioning in Canberra, Copenhagen and Tokyo. *Global Food Security*, 3, 1-7. <https://doi.org/10.1016/j.gfs.2013.09.001>
- Prain, G., & Lee-Smith, D. (2010). Urban agriculture in Africa: What has been learned? In G. Prain, N. Karanja, & D. Lee-Smith (Eds.), *African Urban Harvest. Agriculture in the cities of Cameroon, Kenya and Uganda* (pp. 13-35). New York: Springer.
- Rahman, M. (2016). Detection of land use/land cover changes and urban sprawl in Al-Khobar, Saudi Arabia: An analysis of multi-temporal remote sensing data. *ISPRS International Journal of Geo-Information*, 5(2), 15.
- Richards, J. A. (1999). *Remote sensing digital image analysis: An introduction*. (5th ed.) Berlin: Springer.
- Robson, J.S., Ayad, H.M., Wasfi, R.A., & El-Geneidy, A.M. (2012). Spatial disintegration and arable land security in Egypt: A study of small- and moderate-sized urban areas. *Habitat International*, 36, 253-260. <https://doi.org/10.1016/j.habitatint.2011.10.001>
- Ruelland, D., Levvasseur, F., & Tribotté, A. (2010). Patterns and dynamics of landcover changes since the 1960 over three experimental areas in Mali. *International Journal of Applied Earth Observation and Geoinformation*, 12S, S11-S17. <https://doi.org/10.1016/j.jag.2009.10.006>
- Seto, K. C., & Ramankutty, N. (2016). Hidden linkages between urbanization and food systems. *Science*, 352(6288), 943-945. <https://doi.org/10.1126/science.aaf7439>
- Sexton, J. O., Song, X. P., Huang, C., Channan, S., Baker, M. E., & Townshend, J. R. (2013). Urban growth of the Washington, DC–Baltimore, MD metropolitan region from 1984 to 2010 by annual, Landsat-based estimates of impervious cover. *Remote Sensing of Environment*, 129, 42-53.
- Shalaby, A., & Moghanm, F. S. (2015). Assessment of urban sprawl on agricultural soil of northern Nile delta of Egypt using RS and GIS. *Chinese Geographical Science*, 25(3), 274-282. <https://doi.org/10.1007/s11769-015-0748-z>
- Singh, A., (1989). Digital change detection techniques using remotely sensed data. *International Journal of Remote Sensing*, 10, 989–1003. <https://doi.org/10.1080/01431168908903939>
- Tawk, S. T., Moussa, Z., Abi Saiid, D. M., Abi Saiid, M., Hamadeh, S. (2011). Redefining a sustainable role for urban agriculture in the Middle East and North Africa. *Urban agriculture in the Mediterranean*, Watch Letter n° 18, 1-4. Bari: CIHEAM.
- Thebo, A. L., Drechsel, P., Lambin, E. F. (2014). Global assessment of urban and peri-urban agriculture: irrigated and rainfed croplands. *Environmental Research Letters*, 9, 114002, <https://doi.org/10.1088/1748-9326/9/11/114002>
- UNDP (2009). *Arab Human Development Report*. Challenges to Human Security in the Arab Countries. New York: United Nations Development Programme, Regional Bureau for Arab States (RBAS).
- UN-Habitat (2014). *The state of African cities 2014. Re-imagining sustainable urban transitions*. Nairobi: United Nations Human Settlements Programme (UN-Habitat).
- UNRWA (2019). Statistics of United Nation Relief and Works Agency for Palestine Refugees in the Near East. <https://www.unrwa.org/where-we-work/jordan> Accessed 09 April 2019.
- Veninga, W., & Ihle, R. (2018). Import vulnerability in the Middle East: effects of the Arab spring on Egyptian wheat trade. *Food Security*, 10, 183-194. <https://doi.org/10.1007/s12571-017-0755-2>
- Vorovencii, I., & Muntean, M.D., (2013). Evaluation of supervised classification algorithms for Landsat 5 TM images, *RevCAD*, 14/2013, 197-206.

- Wakode, H. B., Baier, K., Jha, R., & Azzam, R. (2014). Analysis of urban growth using Landsat TM/ETM data and GIS—a case study of Hyderabad, India. *Arabian Journal of Geosciences*, 7(1), 109-121
- Yagoub, M. M. (2004). Monitoring of urban growth of a desert city through remote sensing: Al-Ain, UAE, between 1976 and 2000. *International Journal of Remote Sensing*, 25(6), 1063-1076.
- Zhou, D., Matsuda, H., Hara, Y., & Takeuchi, K. (2012). Potential and observed food flows in a Chinese city: a case study of Tianjin. *Agriculture and Human Values*, 29, 481-492. <https://doi.org/10.1007/s10460-012-9374-x>

List of Tables

Table 1. Major characteristics of the case study cities Luxor and Cairo in Egypt and Aqaba and Amman in Jordan.

Table 2. Summary of satellite images used in the study of four cities in the MENA region.

Table 3. Overview of land cover classes applied for each of the four cities in the MENA region.

Table 1. Major characteristics of the case study cities Luxor and Cairo in Egypt and Aqaba and Amman in Jordan.

City	Area (km ²)	Population (2017-2018)	Altitude (m asl)	Coordinates	Mean annual temp. (°C)	Mean summer temp. (°C)	Mean rainfall (mm yr ⁻¹)	Climate*
Luxor	714	1,300,000	76	25°41'N 32°39'E	24.6	40.0	0	BWh
Cairo	3,085	9,570,441	29	30°08'N 31°24'E	21.3	34.0	18	BWh
Aqaba	375	198,500	24	29°31'N 35°0'E	24.6	35.0	32	BWh
Amman	7,579	4,226,700	857	31°59'N 35°59'E	16.6	31.0	350	BSh

Source: <https://www.weatherbase.com/>, * Climate according to Köppen-Geiger classification

Table 2. Summary of satellite images used in the study of four cities in the MENA region.

City	Date	Landsat No.	Scanner	Pixel Size (m)
Luxor (path/row: 175/42)	30-06-1975	2	MSS	60*60
	06-06-1984	5	TM	30*30
	26-06-1990	5	TM	30*30
	08-08-2000	5	TM	30*30
	17-06-2011	5	TM	30*30
	07-06-2018	8	OLI/TIRS	30*30
Cairo (path/row: 176/39)	31-08-1972	1	MSS	60*60
	02-07-1984	5	TM	30*30
	03-07-1990	5	TM	30*30
	30-07-2000	5	TM	30*30
	13-07-2011	5	TM	30*30
	16-07-2018	8	OLI/TIRS	30*30
Aqaba (path/row: 174/40)	29-06-1975	2	MSS	60*60
	04-07-1984	5	TM	30*30
	21-07-1990	5	TM	30*30
	16-07-2000	5	TM	30*30
	15-07-2011	5	TM	30*30
	16-06-2018	8	OLI/TIRS	30*30
Amman (path/row: 174/38)	29-06-1975	2	MSS	60*60
	18-06-1984	5	TM	30*30
	18-05-1990	5	TM	30*30
	29-05-2000	5	TM	30*30
	12-07-2011	5	TM	30*30
	02-07-2018	8	OLI/TIRS	30*30

Table 3. Overview of land cover classes applied for each of the four cities in the MENA region.

Luxor	Cairo	Aqaba	Amman
Urban (buildings, roads)	Urban (buildings, roads)	Urban (buildings, roads, industrial area, harbour)	Urban (buildings, roads)
Peri-Urban Green (shrub, agricultural land)	Peri-Urban Green (shrubs, agricultural land)	Peri-Urban Green (shrubs, agricultural land)	Peri-Urban Green (shrubs, forests, agricultural land)
-	Urban+green (buildings, gardens and shrubs)	-	Urban+green (buildings, gardens and shrubs)
Desert/barren	Desert/barren	Mountain/barren	Mountain/barren

List of Figures

Fig. 1. Study areas of Luxor and Cairo in Egypt.

Fig. 2. Study areas of Aqaba and Amman in Jordan.

Fig. 3. Changes of peri-urban green areas in Luxor (Egypt) from 1984 to 2018.

Fig. 4. Results of a supervised classification of land use for Luxor in 2000 using SAM algorithm by QGIS (left) and MLC by R coding (right).

Fig. 5. Changes of peri-urban green area in Amman (Jordan) from 1984 to 2018.

Fig. 6. Land cover changes over five decades in Luxor and Cairo, Egypt.

Fig. 7. Land cover changes over five decades in Aqaba and Amman, Jordan.

Fig. 8. Area changes (a+d), percentage changes (b+e) and per-capita changes (c+d) of different land cover classes over the last five decades in Luxor and Cairo, Egypt.

Fig. 9. Area changes (a+d), percentage changes (b+e) and per-capita changes (c+d) of different land cover classes over the last five decades in Aqaba and Amman, Jordan.

Fig. 10. Per capita imports of wheat in Egypt and Jordan from 1961 to 2016.

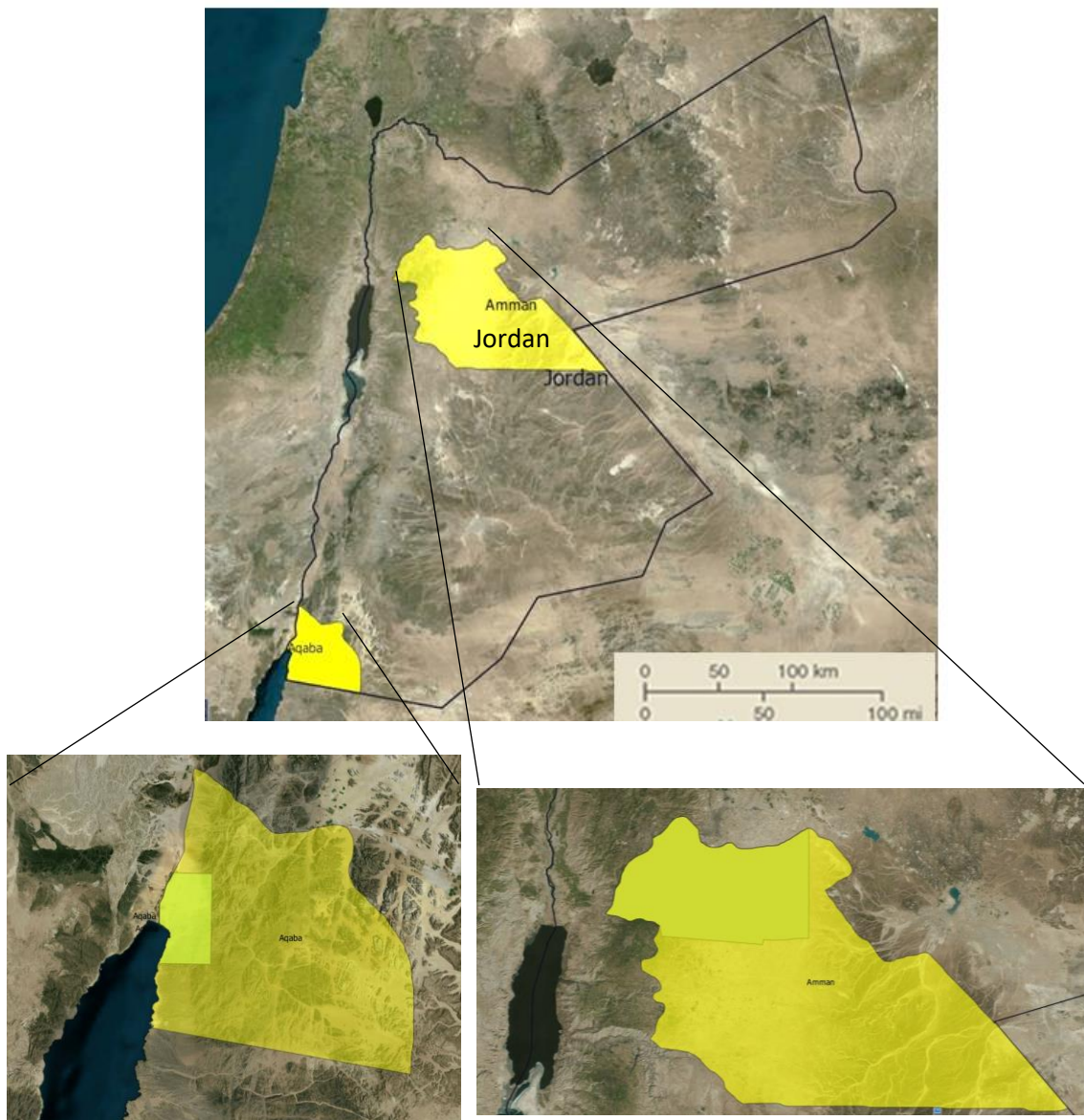


Fig. 2. Study areas of Aqaba and Amman in Jordan (Source: Google Earth).

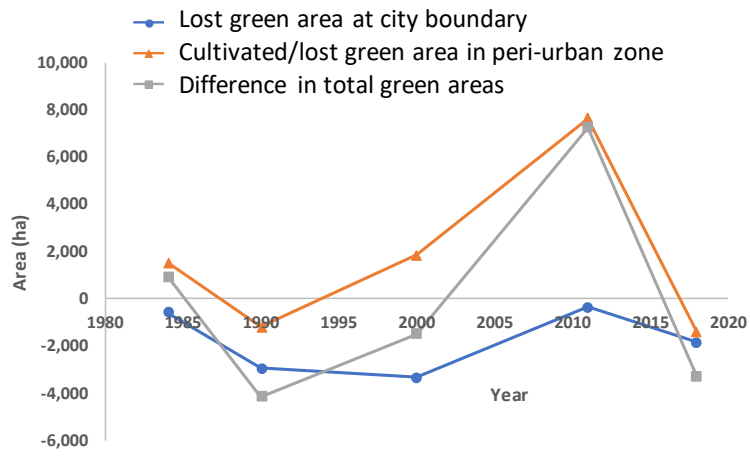


Fig. 3. Changes of peri-urban green areas in Luxor (Egypt) from 1984 to 2018.

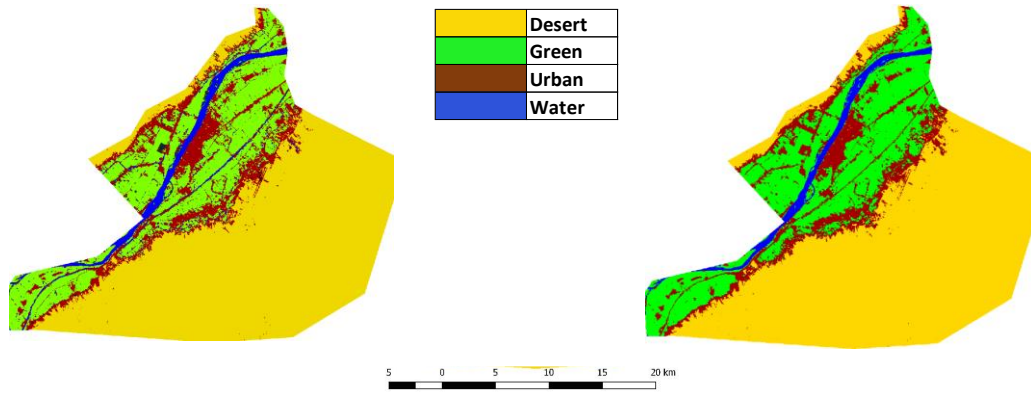


Fig. 4. Results of a supervised classification of land use for Luxor in 2000 using SAM algorithm by QGIS (left) and MLC by R coding (right).

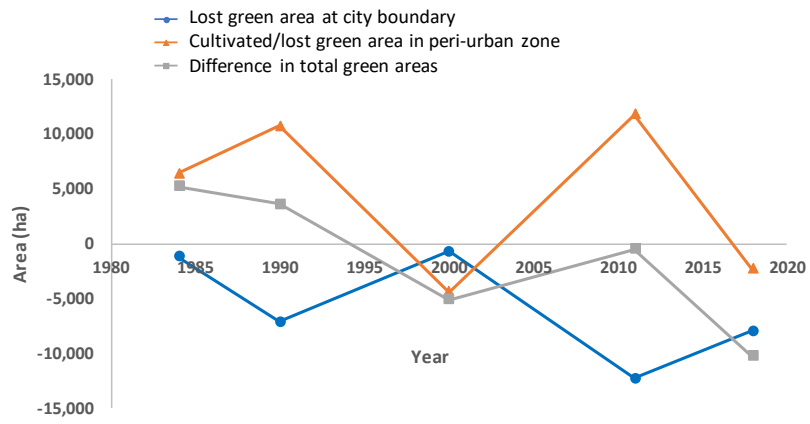
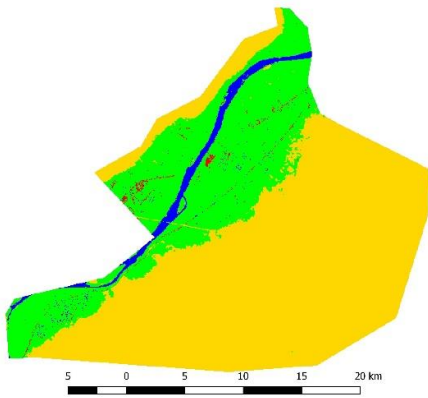
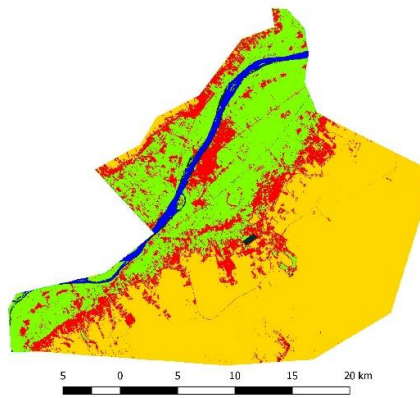


Fig. 5. Changes of peri-urban green area in Amman (Jordan) from 1984 to 2018.

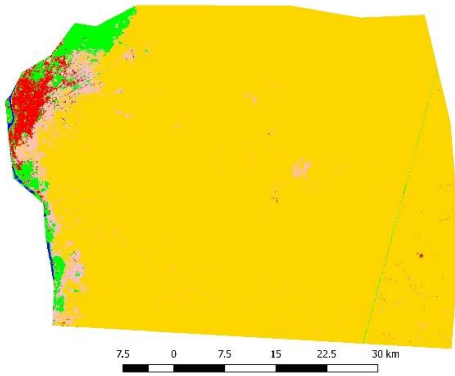
a) Luxor 1975



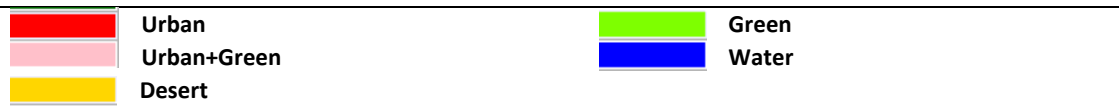
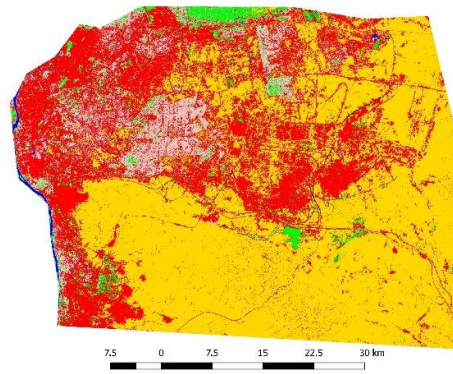
b) Luxor 2018



c) Cairo 1972



d) Cairo 2018

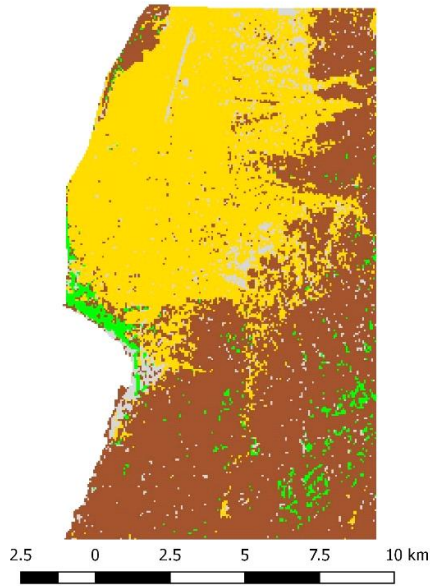


WGS 1984
UTM Zone 36N

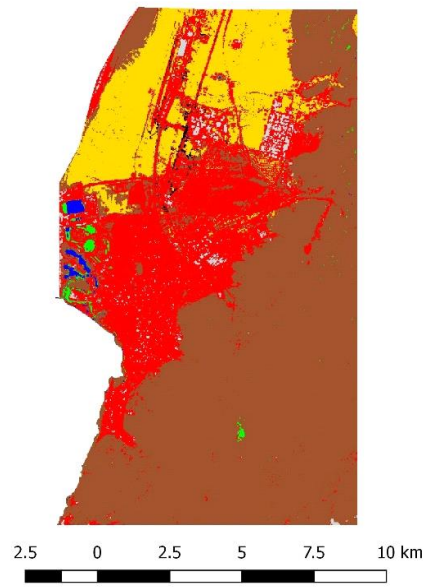


Fig. 6. Land cover changes over five decades in Luxor and Cairo, Egypt.

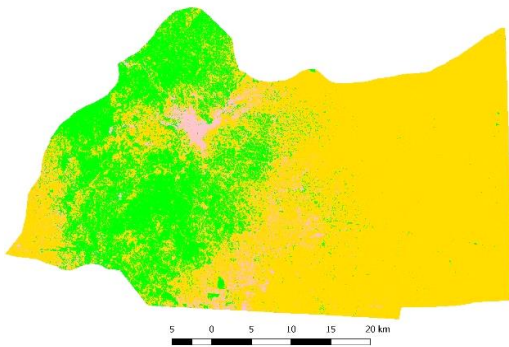
a) Aqaba 1975



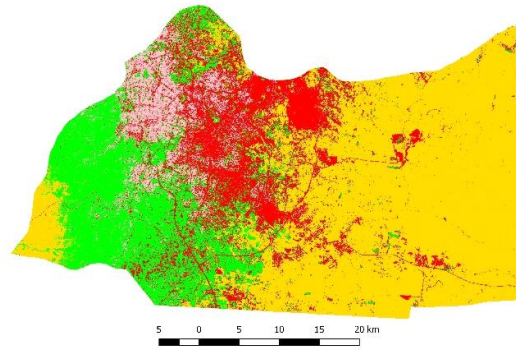
b) Aqaba 2018



c) Amman 1975



d) Amman 2018



WGS 1984
UTM Zone 36N



Fig. 7. Land cover changes over five decades in Aqaba and Amman, Jordan.

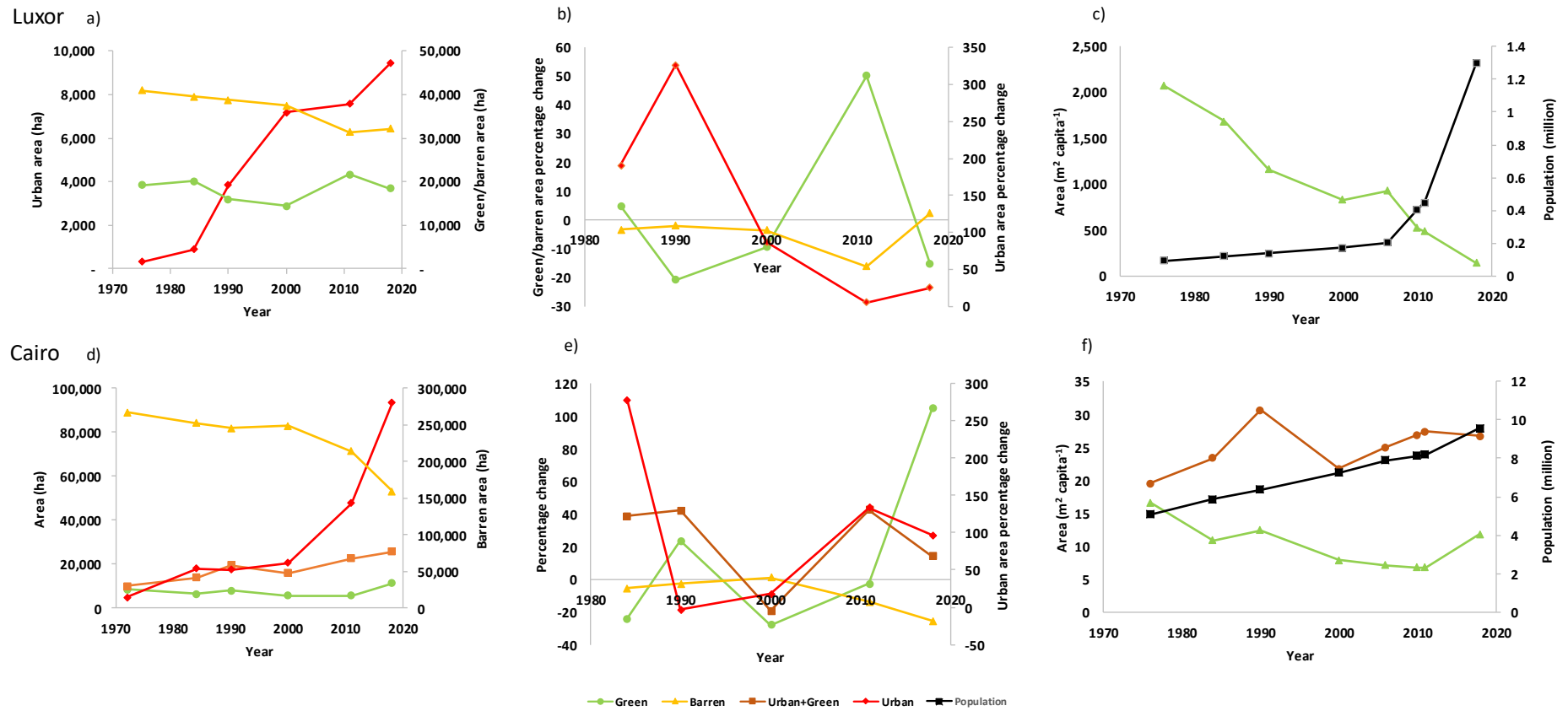


Fig. 8. Area changes (a+d), percentage changes (b+e) and per-capita changes (c+f) of different land cover classes over the last five decades in Luxor and Cairo, Egypt.

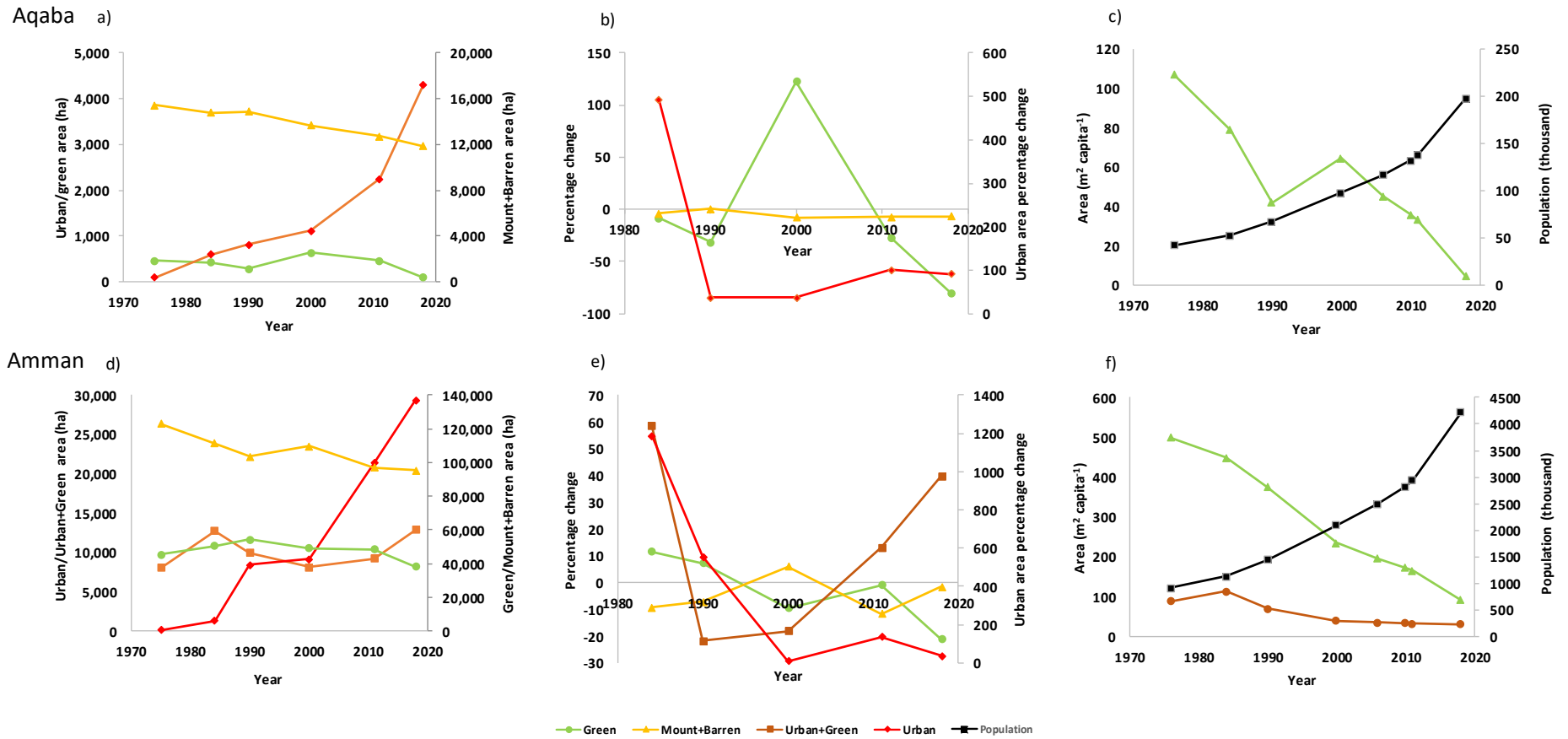


Fig. 9. Area changes (a+d), percentage changes (b+e) and per-capita changes (c+d) of different land cover classes over the last five decades in Aqaba and Amman, Jordan.

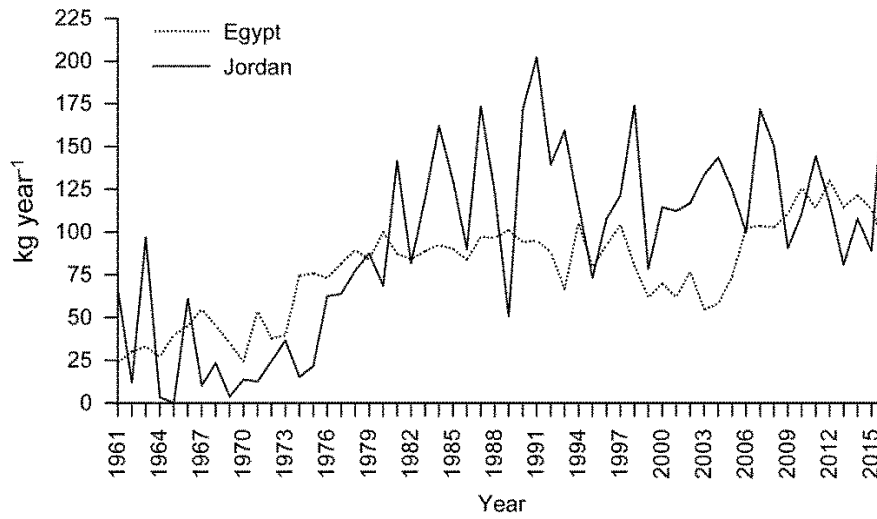


Fig. 10. Per capita imports of wheat in Egypt and Jordan from 1961 to 2016 (Source: www.fao.org/faostat/ and <https://data.worldbank.org/>).